Parametric Variation for Detailed Model of External Grid in Offshore Wind Farms

Vladimir Myagkov*, Lennart Petersen†, Saioa Burutxaga Laza‡, Florin Iov§, Lukasz Hubert Kocewiak¶
*†‡§Department of Energy Technology, Aalborg University. ¶DONG Energy. Denmark
Email: *mjagkow@hotmail.com, †le.petersen@gmx.de, ‡saioa.burutxaga.laza@gmail.com, §fi@et.aau.dk,
¶lukko@dongenergy.dk

***Abstract*—The representation of the external grid impedance is a key element in harmonic studies for offshore wind farms. The external grid impedance is here represented by two different approaches: by a simplified impedance model, based on values for short-circuit power and XR-ratio and by locus diagrams given for a range of harmonic orders. Harmonic studies are carried out with these two different representations and their results are compared subsequently, giving information about the specifity of data that is required for assessing the worst case resonances. This analysis provides the basis for defining a procedure for conducting harmonic studies in wind farms that can be used in commercial project developments.**

***Index Terms*—external grid, wind energy, offshore wind farm, wind turbine, harmonic analysis, grid codes.**

I. Introduction

OFFSHORE wind farms (OWFs) are being connected to national transmission grids. The integration of these renewable generation plants into present power systems poses challenges that must be tackled in order to preserve the correct operation of the system. A clear example of these challenges are the harmonic issues implied in the high voltage alternating current (HVAC) connection of large OWFs.

In frequency domain studies resonances between capacitive elements of the OWF and inductive elements of the system (e.g. external grid, transformers) can be a problem. If a resonance point hits the frequency of a certain harmonic that is present in the system, the resonance impedance could effectively amplify the harmonic above acceptable limits [1]. These harmonic distortion limits are stated in local grid codes and are defined at the point of common coupling (PCC) between the OWF and the external grid (EG).

Therefore, OWF operators should include necessary equipment (e.g. filters) to ensure the functioning of the system in accordance with the grid codes. For the proper design of this equipment harmonic analysis of the system is carried out by means of simulations [2]. In these harmonic studies the representation of the EG impedance is of great importance.

Transmission system operators (TSO) and distribution network operators (DNO) provide different grid impedance models for harmonic studies. In most cases the EG impedance at a PCC is only estimated for the fundamental frequency based on the short-circuit ratio at the corresponding voltage level [3]. However, harmonic resonances are influenced by the frequency dependent grid impedance. In this way, different representations of the EG impedance may lead to different results regarding the impedance at the PCC and thus to different harmonic resonances where voltage distortions may occur.

In this study the EG impedance is represented by two different approaches: by a simplified impedance model and by grid locus diagrams. By using the simulation tool *PowerFactory,* harmonic studies are carried out for a generic, but realistic, OWF with these two different representations and their results are compared. This analysis provides the basis for defining a methodology for conducting harmonic studies in OWFs in order to identify realistic conditions that lead to the worst case harmonic distortions and to investigate and propose feasible mitigation methods.

The rest of this paper is organized as follows: Section II describes the composition of the applied benchmark OWF and the relevant grid code requirements for this study. Section III outlines the modelling approach for the OWF components, whereby Section IV focusses on the EG representation. The simulation results are presented in Section V, which leads to a proposed methodology for harmonic assessment in Section VI.

II. System Description and Requirements

A. System Characterization of the Benchmark Wind Farm Network

A benchmark OWF located in United Kingdom is used as a base case for this study. The OWF is designed taking into account the requirements for transmission systems in UK and general engineering rules for OWF topologies. The OWF topology is presented in Fig. 1. It comprises 50 wind turbine generators (WTGs) of variable speed, full-scale power converter and a rated power of 3.6 MW. The OWF power is transferred to the onshore grid by an export cable, where the PCC is defined.

B. Grid Code Requirements

The UK grid code [4] sets the principles for operating power plants, determining the relationship between the National Grid Transmission System (NGET) and all users of the National Electricity Transmission System (NETS). Regarding voltage waveform quality requirements, OWFs in UK should follow the planning criteria stated in the *Engineering Recommendation G5/4* [5]. The power plant operator should fulfill the planning

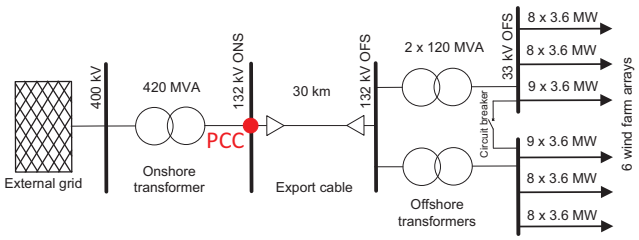

Figure 1. Single line diagram of benchmark offshore wind farm

levels at the PCC defined for the voltage waveform distortions due to harmonic content.

III. Modelling of Wind Farm Components for Harmonic Studies

A. Wind Turbine Generator's Harmonic Emissions

In order to evaluate the planning levels at the PCC, it is essential to model the harmonic emissions of the WTGs in the most appropriate manner. According to [6] harmonic currents are produced by power electronic converters in WTGs due to the switching operation. The common representation of the WTG used for harmonic load flow assessments is shown in Fig. 2.

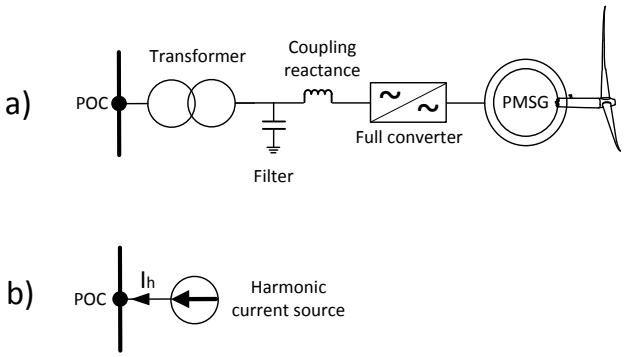

Figure 2. Wind turbine harmonic representation, a) topology of type-4 wind turbine acc. to [7], b) representation as harmonic current source acc. to [8]

In Fig. 2 a) the WTG topology is depicted, where a permanent magnet synchronous generator (PMSG) generates power, which is transferred by a full-scale converter. Then according to [8] the operating principle of a converter can be described by a harmonic voltage source, as it defines the output voltage waveform U_h by its switching operation. As a result a harmonic current I_h will flow towards the point of connection (POC). If the harmonic current spectrum is known, the whole WTG may be represented as a harmonic current source as illustrated in Fig. 2 b).

In this study these harmonic emissions are included in the simulation model by representing WTGs as harmonic current sources. The harmonic emissions of the *Enercon E-82-E2* WTG are used [9]. Since it features a type-4 WTG, it is applied for a simplified assumption of harmonic emissions. The maximum harmonic emissions related to the rated current of this WTG are shown in Fig. 3.

B. Cables

For representing cables by equivalent circuits there are different line models available, as for instance the lumped and the distributed parameter model. The relation of physical and wave length of the cable defines which model shall be applied for investigations in harmonic domain [10]. The wave length is dependent on the corresponding inductance L' and capacitance C' per unit length of the cable. The wave length λ_{line} is calculated according to eq. 1 for the highest frequency to be evaluated.

$$\lambda_{line} = \frac{1}{f \cdot \sqrt{L' \cdot C'}} \tag{1}$$

Lines may be modelled with lumped parameters, if their physical length is not of the same order of magnitude as the length of wave of the voltage or current at the frequency under consideration [10]. In this study, the OWF's array cables are modelled by the π-model with lumped parameters. On the other hand, the export cable length is of the same order of magnitude as the voltage wave, hence it is modelled by distributed parameters. [11]

C. Transformers

The transformers are respresented by their power rating and internal impedance under normal operating conditions. The magnetization current of the transformers is not taken into account, since it is low at nominal voltage. Therefore, the WTGs are the only harmonic sources in the OWF network.

IV. External Grid Representation

A. Simplified Impedance Model

In the *Electricity Ten Year Statement* of *National Grid* there are presented the fault levels for various locations in the UK grid [12]. The fault currents at grid voltages of $U_{grid} = 400\,\mathrm{kV}$ vary between $I_{k,min} = 5.5\,\mathrm{kA}$ and $I_{k,max} = 47.7\,\mathrm{kA}$ for all the listed locations. According to eq. 2 the resulting range for the short-circuit power results to $S_{k,min} = 3776\,\mathrm{MVA}$ and $S_{k,max} = 33048\,\mathrm{MVA}$ and hence for the grid impedance to $Z_{k,max} = 42.4\,\Omega$ and $Z_{k,min} = 4.8\,\Omega$.

$$S_k = \sqrt{3} I_k U_{grid} = \frac{U_{grid}^2}{Z_k} \tag{2}$$

A common value for the XR-ratio recommended in grid codes and used in studies ([13], [14]) is 10 and is also applied in this investigation. Hence, the EG of the connected OWF may be interpreted as stiff with $XR = 10$. According to equations 2

to 4 the necessary design parameters for the EG, depending on the ranges of S_k and XR, are summarized.

$$R_k = \sqrt{Z_k^2 - X_k^2} = \frac{Z_k}{\sqrt{1 + XR^2}} \quad (3)$$

$$X_k = XR \cdot R_k \quad (4)$$

B. Frequency Dependent Impedance

In order to represent the EG as realistic as possible in the harmonic domain, frequency dependent impedances are implemented. Impedance plots in terms of locus diagrams are provided by *National Grid* for harmonic orders of the range of $2 \leq \mathrm{h} \leq 17$, taking into account various impedance values the EG can feature dependent on the system configuration and operation. The later assessment is limited to these orders. The impedance locus for harmonics from the 2^{nd} to the 5^{th} and from the 6^{th} to the 17^{th} order are respectively described by the shaded area in Fig. 5. The resistance and reactance are given in per-unit based on the fundamental impedance of the EG.

C. Background Harmonics

The background voltage distortion is represented by values in % of the fundamental voltage for different harmonic orders. Data are again provided by *National Grid* as an exemplary study case and shown in Fig. 3.

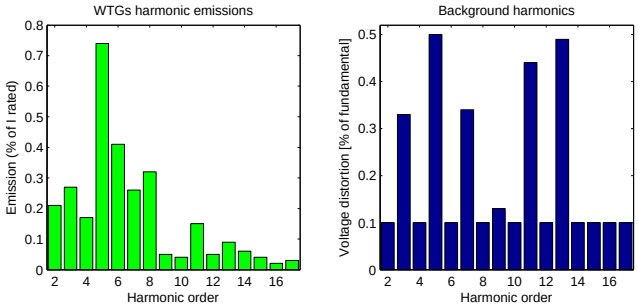

Figure 3. Left: Wind turbine generator's harmonic current emissions in % of rated current from *Enercon E-82-E2*; Right: Background voltage distortion $U_{h,grid}$ in % of the fundamental voltage [15]

Then, the harmonic voltage distortion at the PCC will be determined by the interaction between the background harmonics, the harmonics emitted by the WTGs and the aggregated impedance characteristic at that point in the network.

V. Results

Studies in harmonic domain are performed for assessing the impact of harmonic distortions at the PCC. To this aim, both EG impedance models are implemented in the *PowerFactory* simulations.

In this paper only the results obtained with $S_{k,min}$ are presented as an exemplary case. However, using $S_{k,max}$ has led to comparable findings. [11]

A. Frequency Dependent Impedance

For the frequency dependent impedance representation, an algorithm is prepared for conducting a series of *Frequency Sweep* and *Harmonic Load Flow* simulations. From the 2^{nd} harmonic order up to the 17^{th}, the script modifies the EG impedance according to the geometrical characteristics of the predefined locus diagrams, shown in Fig. 5, in iterative simulations. The impedance $Z_{h,PCC}$ and maximum harmonic distortion $U_{h,PCC,max}$ at the PCC are calculated for each harmonic order.

The dependency of the simulated impedance $Z_{h,PCC}$ at the PCC on various R and X values of the grid locus is explained by Fig. 4. The $Z_{h,PCC}$ is exemplary shown for four different harmonic orders, simulated for $S_{k,min}$.

For $h = 2$ the impedance amounting to $Z_{2,PCC} = 14\,\Omega$ is totally independent of the values inside the grid locus. For $h = 3$ the highest impedance $Z_{3,PCC} = 26.5\,\Omega$ is calculated for a maximum grid reactance of $X_{grid} = 0.6\,\mathrm{pu}$, yet independent on the change of R_{grid}. But the relatively small range of $\Delta Z_{3,PCC} = 6\,\Omega$ does not indicate a significant influence by the grid locus on the resulting impedance. Similar results as in a) and b) of Fig. 4 can be obtained for all harmonic orders excluding the 6^{th} and 7^{th} order, which is attributed to the non-occurrence of resonances at those frequencies being less affected by changes of the grid impedance.

For $h = 6$ the highest impedance $Z_{6,PCC} = 600\,\Omega$ occurs at maximum $X_{grid} = 4.7\,\mathrm{pu}$ and at low $R_{grid} = 0.35\,\mathrm{pu}$, which points to a low damping of the parallel resonance. The rise in impedance at this point indicates a resonance that can cause high harmonic distortion. The great span of possible values inside the grid locus causes duplication of this resonance point at $h = 7$. It can be detected at a lower grid reactance. $X_{grid} = 1.62\,\mathrm{pu}$ and the corresponding lowest resistance $R_{grid} = 0.017\,\mathrm{pu}$. The relatively wide ranges of the simulated impedance $\Delta Z_{6,PCC} = 500\,\Omega$ in Fig. 4 c) and $\Delta Z_{7,PCC} = 4000\,\Omega$ in Fig. 4 d) justifies that the points of the grid locus have to be checked thoroughly in order to observe the worst case resonances. Particularly the result of Fig. 4 d) shows that specific points of the grid locus lead to high resonance impedance, whereas points in the vicinity do not.

Fig. 5 shows for all scenarios and harmonic orders the locations inside the grid locus leading to the highest harmonic distortion $U_{h,PCC}$ at the PCC. Harmonic orders, which indicate no dependency on R_{grid} and X_{grid} like for Fig. 4 a), are excluded. The result points out that the extreme values are located on the boundary of the grid locus. This behaviour implies that it is sufficient for harmonic studies to sample the boundary values of a certain grid locus in order to determine the worst case impedances, which lead to the highest harmonic distortions. Hence, the simulation time can be shortened without obtaining inadequate results.

B. Comparison of Both Grid Representations

For the simple EG impedance representation the R_k and X_k values, corresponding to $S_{k,min}$ and $XR = 10$, are

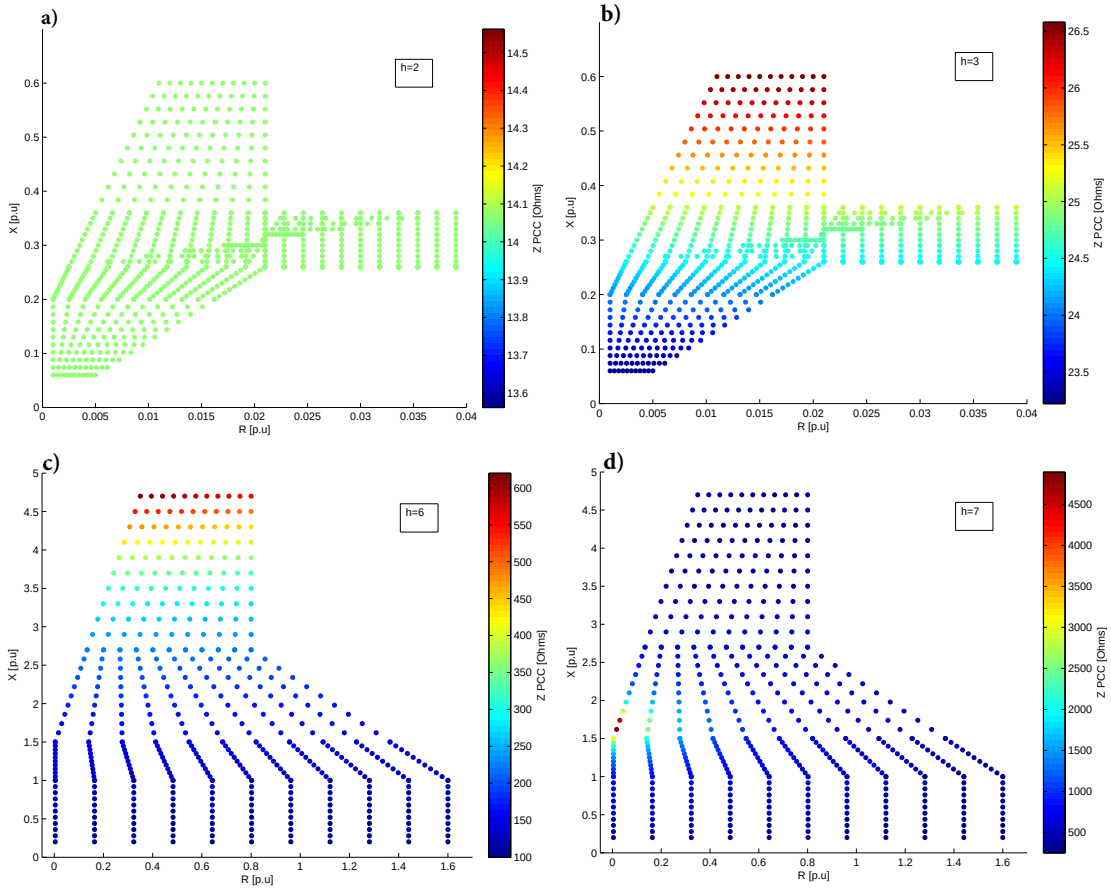

Figure 4. Simulated impedance $Z_{h,PCC}$ at PCC as a function of possible R_{grid} and X_{grid} values of the grid locus, for $S_{k,min}$ and different harmonic orders: a) $h = 2$, b) $h = 3$, c) $h = 6$, d) $h = 7$

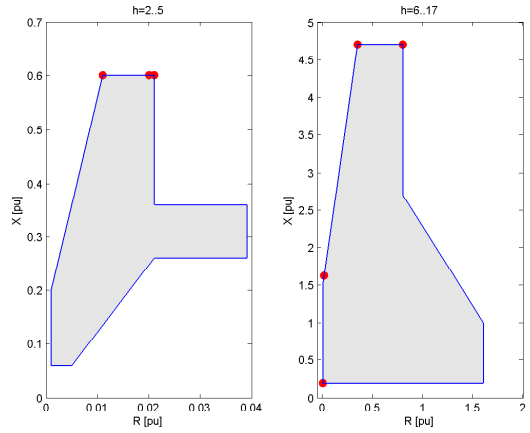

Figure 5. Locations inside the grid locus leading to the highest harmonic distortion $U_{h,PCC}$ at the PCC, for all scenarios and those harmonic orders indicating variations in $Z_{h,PCC}$ along the grid locus area

implemented in *PowerFactory* to carry out the same harmonic studies.

In Fig. 6 the frequency dependent impedance characteristics at the PCC is depicted, taking into consideration the worst case impedances $Z_{h,PCC}$ obtained by sampling the impedance area of the corresponding grid locus. Here, the $Z_{h,PCC}$ characterictics obtained with the two different EG representations can be easily compared. In Fig. 6 it is important to highlight that the duplication of the resonance point at $h = 6$ and $h = 7$ leads to high impedances at both orders (green bars) as already explained by Fig. 4. The differences between both grid representations are significant at these orders. Hence, it is worth analyzing the harmonic distortions for these scenarios as illustrated in Fig. 7.

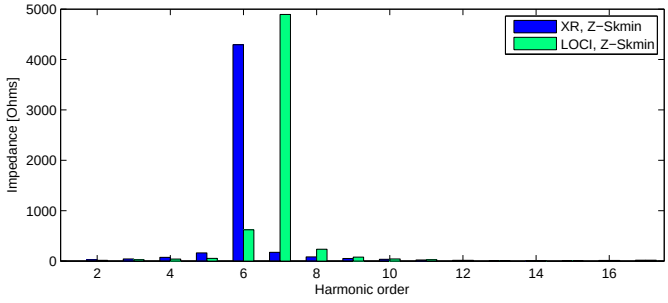

Figure 6. Frequency dependent impedance at PCC, presented in integer steps from 2^{nd} to 17^{th} harmonic order, for short-circuit power level $S_{k,min}$, comparing the grid representation by short-circuit power level (blue) and by worst case impedance of grid locus diagram (green)

It can be observed for $h = 6$ that the limits are exceeded for both cases. However, the more detailed representation by the grid locus implies a lower harmonic distortion ($\Delta U_6 = 10\,\%$). On the other hand, for $h = 7$ the sophisticated model of the EG implies a significantly higher harmonic distortion ($\Delta U_7 = 33\,\%$). Here, the resonance point causes non-compliance with the limits, whereas by using the simplified representation of the EG impedance, one would mistakenly assume that the limits are observed.

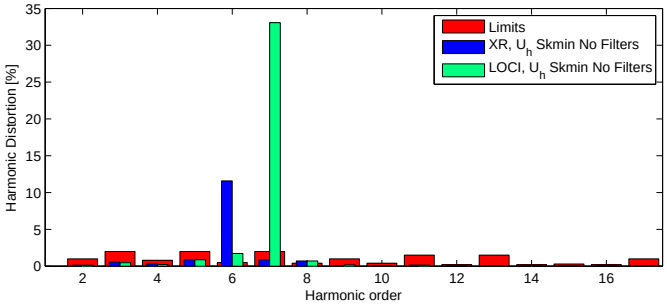

Figure 7. Harmonic distortions at PCC from 2^{nd} to 17^{th} harmonic order, for short-circuit power level $S_{k,min}$, comparing the grid representation by short-circuit power level (blue) and by grid locus diagram (green), and harmonic limits stipulated by [5] (red)

Subsequently it is assessed whether the same filter equipment can be aplied for both EG impedance representations. In this study harmonic mitigation is approached by using passive filters, more precisely single-tuned filters [16]. These filters composed by a series connection of R-L-C are tuned to a specific harmonic frequency, which offer low impedance Z_{filter} and can be expressed by eq. 5 with the series components R_s, X_L and X_C at nominal frequency.

$$Z_{filter} = R_s + j(X_L + X_C) = R_s + j(\omega \cdot L - \frac{1}{\omega \cdot C}) \quad (5)$$

Single-tuned filters are designed at 132 kV onshore busbar for the 6^{th} and 8^{th} orders. By filtering these two harmonics, a mitigation effect likewise on the 7^{th} harmonic is expected to be achieved.

Harmonic distortions with the proposed single-tuned filters are shown in Fig. 8, allowing a comparison of both grid representations.

The grid code requirements are fulfilled for all considered harmonic orders. As expected, since the passive filters are tuned for the 6^{th} and 8^{th} order, the harmonic distortions at these orders are mitigated. Even the 7^{th} harmonic is lowered to the extent that it comes below the limit. This is due to the characteristic of both filters, which damp impedances in the near vicinity of the tuned order. Therefore, also the total harmonic distortion (THD) level is kept below the limit of 3%. Hence, in this case the design of filter equipment is valid for both EG impedance representations. However, in other study cases, e.g. for various shapes of locus diagrams, resonance frequencies may occur at frequencies which differ widely from

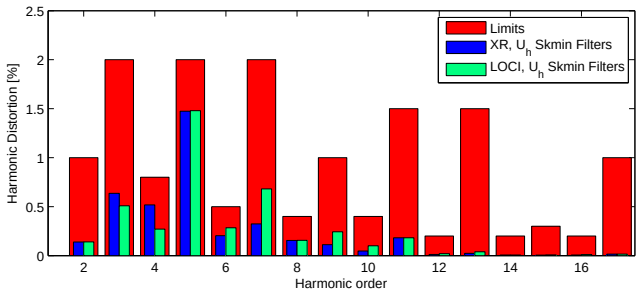

Figure 8. Harmonic distortions at PCC from 2^{nd} to 17^{th} harmonic order, for short-circuit power level $S_{k,min}$ and after implementation of filter equipment, comparing the grid representation by short-circuit power level (blue) and by grid locus diagram (green), and harmonic limits stipulated by [5] (red)

the ones detected by the simplified representation. Hence, it is preferable to perform harmonic studies by having a detailed model of the EG, before equipment for harmonic mitigation is scrutinized.

VI. Proposal of Methodology for Conducting Harmonic Studies

Based on the results presented, a methodology for the detection and mitigation of harmonic voltage distortion at PCC can be conceptualized by the algorithm given in Fig 9. With this algorithm all the scenarios under study are considered and for each of them it is ensured that the harmonic distortion limits are not exceeded in a certain frequency spectrum. The number of scenarios N depends on various configurations of the OWF. As for instance, the OWF power at partial load may be transferred by having only one offshore transformer in operation.

The base stage of this methodology is to identify the data available regarding the representation of the EG impedance. If locus diagrams are available for a frequency range, then the harmonic studies are performed taking into account this information. Hence, usage of S_k and XR-ratio should be applied for simulations only for the remaining harmonic orders, for which no data is provided or, if locus diagrams are not available at all.

The harmonic analysis begins by calculating the frequency dependent impedance characteristic of the PCC in order to evaluate the resonances that may appear. When locus diagrams are available, only the impedance values on the chart boundaries are considered, as this study has shown the sufficiency of using these values. This stage is then followed by a harmonic load flow simulation, which allows the identification of the exceeded limits, if any, and provides information for the design of filters contributing to mitigate the resonances causing these harmonic voltage distortions. These steps are performed for all defined scenarios in order to observe critical resonances and harmonic distortions for all possible OWF configurations.

Once the filters are implemented, frequency sweeps and harmonic load flow simulations shall prove that the distortion limits are no longer exceeded. If they do, the filters have to be redesigned. When the critical resonances are mitigated, it is

considered that, even for the worst harmonic distortion cases, the system complies with grid code requirements regarding harmonic distortions. Therefore, the harmonic analysis of the system is concluded at this point.

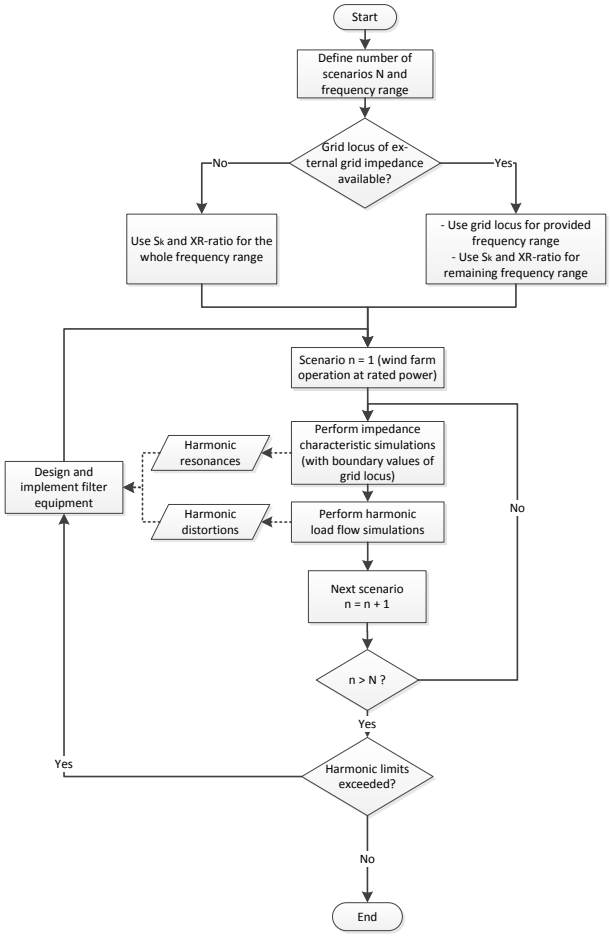

Figure 9. Algorithm for harmonic studies in offshore wind farms

VII. Conclusion

Using the simulation results comparing a simplified and more detailed representation of the EG in harmonic domain, this paper has presented a method to identify conditions leading to the worst case harmonic distortions at the PCC of an OWF.

Initially, for a locus representation of the EG, the possible R and X values inside the locus diagrams have been evaluated for each harmonic, resulting in an impedance value and a maximum harmonic voltage at the PCC. The obtained plots show that significant differences for the simulated impedance can be observed only around the resonance frequency depending on the R and X values of the grid locus. Furthermore, it has been ascertained that the impedance values of the grid locus, which lead to maximum harmonic distortions, are always located on the boundaries of the charts. This means that for harmonic investigations the simulation time can be shortened by evaluating only selected points of locus boundary.

By comparing results of the simplified grid representation and the frequency dependent grid impedance, it is observed that different grid representations will lead to different harmonic distortions. A further outcome of this comparison is that by applying the same filter equipment harmonic distortion limits are kept for both grid impedance representation. Nevertheless, if the comparison of resonance frequencies for both grid representations would reveal significant differences, the same single-tuned filters will not damp the critical harmonics obtained by detailed grid modelling.

Acknowlegment

This paper is part of a 1st year MSc project, proposed by DONG Energy. The authors would like to thank Sanjay Chaudhary and Florin Iov from Aalborg University and Lukasz Hubert Kocewiak from DONG Energy for all their support.

References

[1] G. Bathurst R. Hodges, S. Dixon. Management of low frequency resonance for large scale offshore wind power plants with long ac cable connections. *12th wind Integration workshop. International Workshop on Large-Scale Integration of Wind Power into Power Systems as well as on Transmission Networks for Offshore Wind Power Plants*, 22-24 Oct. 2013, London.

[2] K.D. Dettmann D. Schulz. H. Langkowski, Trung Do Thanh. Grid impedance determination. relevancy for grid integration of renewable energy systems. *Industrial Electronics, 2009. IECON '09. 35th Annual Conference of IEEE*, pages 516–521, 2009.

[3] M. Jordan, H. Langkowski, Trung Do Thanh, and D. Schulz. Frequency dependent grid-impedance determination with pulse-width-modulation-signals. *Compatibility and Power Electronics (CPE), 2011 7th International Conference-Workshop*, pages 131–136, 2011 June.

[4] National Grid Electricity Transmission The Grid Code. Issue 5. Revision 6 2013.

[5] Electricity association services. the engineering group. Engineering Recommendation G5/4, February 2001.

[6] Thomas Ackermann. *Wind Power in Power Systems*. Wiley, 2005.

[7] GA Mendonça, HA Pereira, and SR Silva. Wind farm and system modelling evaluation in harmonic propagation studies. In *International Conference on Renewable Energies and Power Quality,(ICREPQ 12), Santiago de Compostela, Spain, March*, volume 28, 2012.

[8] Lukasz Kocewiak. Harmonic analysis of offshore wind farms with full converter wind turbines. *8th International Conference on Large-Scale Integration of Wind Power into Power Systems*, 2009.

[9] M. Bollen M. Whalberg K. Yang, S. Cundeva. Harmonic emission study of individual wind turbines and a wind park. *Renewable Energy and Power Quality Journal.*, ISSN 2172-038 X, 2013.

[10] DIgSILENT GmbH. Technical documentation - overhead line models.

[11] V. Myagkov; L. Petersen; S. Buruchaga Laza. Parametric variation for detailed model of external grid in offshore wind farms. *Semester project report at Aalborg University*, 2014.

[12] National Grid. Electricity ten year statement (etys) 2012 - appendix d - fault levels.

[13] Technical regulation 3.2.5 for wind power plants with a power output greater than 11 kW, 2010.

[14] TN Preda, K Uhlen, DE Nordgard, and T Toftevaag. External grid representation for assessing fault ride through capabilities of distributed generation units. In *Innovative Smart Grid Technologies (ISGT Europe), 2012 3rd IEEE PES International Conference and Exhibition on*, pages 1–9. IEEE, 2012.

[15] National Grid. Generator self build enduring regime harmonic assessment process flow.

[16] SJ Bester and Gary Atkinson-Hope. Harmonic filter design to mitigate two resonant points in a distribution network. In *Universities Power Engineering Conference (AUPEC), 2011 21st Australasian*, pages 1–5. IEEE, 2011.